Comparison of low-P_T photon production in high- and low-multiplicity collisions at the CERN ISR

T. Åkesson,[c] M. G. Albrow,[k] S. Almehed,[m] E. Anassontzis,[l] R. Batley,[c] O. Benary,[p] H. Bøggild,[f] O. Botner,[f] H. Breuker,[c] V. Burkert,[h] B. Callen,[n] R. Carosi,[c] A. A. Carter,[j] J. R. Carter,[b] V. Chernyatin,[d] Y. Choi,[o] W. E. Cleland,[o] S. Dagan,[p] E. Dahl-Jensen,[f] I. Dahl-Jensen,[f] G. Damgaard,[f] B. Dolgoshein,[d] S. Eidelman,[e] C. W. Fabjan,[c] I. Gavrilenko,[g] U. Goerlach,[c] Y. Goloubkov,[d] K. H. Hansen,[f] V. Hedberg,[m] P. Ioannou,[l] G. Jarlskog,[m] T. Jensen,[c] A. Kalinovsky,[d] V. Kantserov,[d] S. Katsanevas,[c] C. Kourkoumelis,[l] R. Kroeger,[o] K. Kulka,[m] D. Lissauer,[p] B. Lorstad,[m] I. Mannelli,[c] A. Markou,[l] S. Mayburov,[g] N. A. McCubbin,[k] R. Møller,[f] W. Molzen,[n] P. Nevsky,[d] B. S. Nielsen,[c] L. H. Olsen,[c] Y. Oren,[p] L. K. Resvanis,[l] J. Schukraft,[c] A. Shemleva,[g] V. Sidorov,[e] H. Specht,[i] I. Stumer,[a] M. Sullivan,[o] H. H. Thodberg,[f] J. A. Thompson,[o] J. Williamson,[k] and W. J. Willis[c]

[a]*Brookhaven National Laboratory, Upton, New York 11973*
[b]*Cambridge University, Cambridge, United Kingdom*
[c]*CERN, Geneva, Switzerland*
[d]*Institute of Moscow Engineering Physics, Moscow, Union of Soviet Socialist Republics*
[e]*Institute of Nuclear Physics, Novosibirsk, Union of Soviet Socialist Republics*
[f]*Niels Bohr Institute, University of Copenhagen, Copenhagen, Denmark*
[g]*P. N. Lebedev Institute of Physics, Moscow, Union of Soviet Socialist Republics*
[h]*Physikalisches Institut, Universitat Bonn, Bonn, Federal Republic of Germany*
[i]*Physikalisches Institut, Universitat Heidelberg, Heidelberg, Federal Republic of Germany*
[j]*Queen Mary College, London, United Kingdom*
[k]*Rutherford Appleton Laboratory, Didcot, United Kingdom*
[l]*University of Athens, Athens, Greece*
[m]*University of Lund, Lund, Sweden*
[n]*University of Pennsylvania, Philadelphia, Pennsylvania 19104*
[o]*University of Pittsburgh, Pittsburgh, Pennsylvania 15260*
[p]*University of Tel Aviv, Tel Aviv, Israel*
(The Axial Field Spectrometer Collaboration)

(Received 28 March 1988; revised manuscript received 30 June 1988)

Low-transverse-momentum photon production at the CERN ISR is compared in high- and low-multiplicity events. High-transverse-energy pp collisions and low-multiplicity $\alpha\alpha$ and pp collisions are studied. Relative photon-to-charged-track production is found to be the same in pp minimum bias, $\alpha\alpha$ minimum bias, and pp high-transverse-energy collisions, to within 15%. No low-P_T excess is seen; the limits are dominated by systematic uncertainties.

I. INTRODUCTION

In a recent article[1] we described our measurement of photon production at low transverse momenta in minimum-bias pp collisions. In that publication we compared two methods of measuring these photons: as conversions, with the electron tracks measured in a drift chamber, and as electromagnetic showers in a NaI calorimeter.

Experiments at lower energies[2,3] have observed an excess compared to what one expects from hadron (π^0, η^0, etc.) decays, attributable to direct photons. Although our study[1] is consistent with the significant excess seen in Ref. 2, the observed photons in our experiment could as well be explained as arising from π^0 and other particle decays. Our data, however, exclude a rapid growth of any direct soft-photon production between center-of-mass energy 12–63 GeV.

One explanation[4] for the excess photons seen in the lower-energy experiments links it with the observed excess of electrons and electron pairs[5–7] through production of virtual photons. Extrapolation to the photon physical mass would then predict a real-photon excess which would grow quadratically with pion multiplicity, as is also predicted for the direct electron pairs. In this explanation, one would then expect enhanced photon production both in heavier-ion collisions and in collisions with large central energy deposition ("high E_T") and thus typically higher multiplicities.

Support for this explanation comes from our group's study of the P_T and multiplicity dependence of the observed positron production at center-of-mass energy 63 GeV (Ref. 5). In the region of P_T 300–400 MeV/c, expected to be dominated by charm decay and hadronic bremsstrahlung, we found a linear increase of positron production with charged-particle multiplicity, consistent with such final-state processes. In the lower-P_T region, <200 MeV/c, the positron yields were a factor of 5

above predictions, and a quadratic dependence on multiplicity was observed, as expected for processes such as parton rescattering,[8] characteristic of intermediate state interactions.[4]

To estimate the real-photon excess, one must know the form of the lepton-pair spectrum.[7,9] Reasonable estimates based on previous measurements give an expected real-photon excess of order π/α times the electron-pair excess. This yields real-photon estimates of order 5% of charged-pion production for low-multiplicity events, ranging up to 20% for the highest multiplicities available in our experiment. The previous measurement, by Chliapnikov *et al.*,[2] of a significant direct photon excess in low-multiplicity events, was consistent with this estimate, but peaked at $P_T < 50$ MeV/c, whereas most models require real-photon transverse momenta of order a few hundred MeV/c. Thus a study of photon production as a function of P_T and multiplicity may constrain the choice of model.

We have therefore measured low-transverse-momentum photon production in higher-multiplicity events, both in $\alpha\alpha$ and high-E_T collisions. The method is to observe the photons as electromagnetic showers in the NaI calorimeter described in Ref. 1. Since the apparatus and analysis procedures are similar to those for the minimum-bias data, the photon yields can be directly compared. In this investigation we are not interested in the absolute photon production, but only the production relative to the charged particles, to search for differences from the minimum-bias case. With this approach, many of the systematic errors cancel. One important source of systematic error is external bremsstrahlung associated with charged tracks. We substantially remove these photons by rejecting photons closely associated with charged tracks.

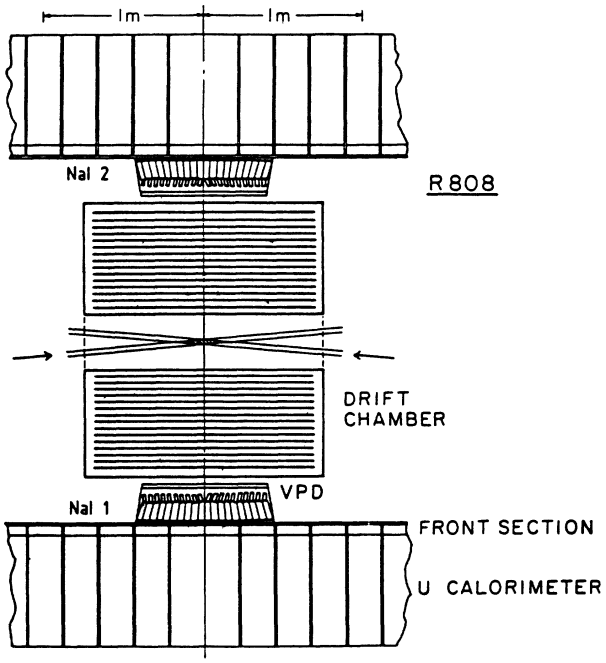

FIG. 1. The central part of the detector, seen from above. The incident beam directions are shown in the center. Photons are detected in the NaI array.

II. APPARATUS

A plan view of the central part of the Axial Field Spectrometer[10] (AFS) is shown in Fig. 1. The important elements of the apparatus for this investigation were the central drift chamber, subtending rapidity ± 1.0, and the NaI photon detectors. There is 4.5% radiation length material in the beam pipe, trigger hodoscope around the beam pipe, and entrance of the drift chamber. The drift-chamber information was used for reconstruction of the charged tracks, which were used for normalization and rejection of fake showers.

The drift chamber operated in an axially symmetric magnetic field of 0.5 T. For a part of the minimum-bias data, the field was reduced to 0.1 T. The chamber was segmented into 82 4° sectors in azimuth: each sector contained 42 sense wires parallel to the bisector of the colliding beams, covering 2π in azimuth except for two 16° wedges in the vertical plane. The coordinates in the transverse plane were provided by drift-time measurements with a spatial resolution of 230 μm and coordinates along the beam direction (z direction) by charge division with 1.5-cm resolution. The momentum resolution is given by $(dp/p)^2=(0.02p)^2+(0.01)^2$, where p is in GeV/c. Over the azimuthal coverage of 328° and for rapidities less than 1, the track acceptance was essentially uniform.

The electromagnetic shower detector is described in detail in Ref. 11. It consisted of two high-granularity walls of NaI crystals. Each wall covered a solid angle of 0.6 sr and consisted of 600 crystals in a 30 (vertical) by 20 (horizontal) matrix. One wall (wall 2) was towards the center-of-mass motion and one (wall 1) was opposite the center-of-mass motion. The 5.3-radiation-length (r.l.) crystals are 3.5 cm by 3.5 cm at the front, approximately 1 m from the intersection region, tapering to 4 cm by 4 cm at the back of the detector. The fraction of photon energy deposited in the NaI crystals, modeled and included in the analysis, is 50–60 % for photons in the range 200 MeV–1 GeV.

The NaI walls and drift chamber were inside a 2π azimuth uranium-scintillator calorimeter of 6-r.l. electromagnetic part and 3.6 absorption lengths hadronic part. This outer calorimeter was used to measure the leakage energy from the NaI, to calibrate the NaI shower detector, and to select the high-E_T events. The NaI detector was calibrated by (1) reconstruction of π^0's from the two-photon decay modes, (2) comparison of electron energy deposition in the NaI with electron momenta measured in the drift chamber, and (3) energy deposition of minimum-ionizing particles in individual crystals. Overall energy calibration for the detector (NaI plus uranium) was determined to within 5%. The response of the NaI alone was determined to within 6% by the consistency of the various methods. A more precise relative calibration of the two NaI walls, to within 2%, was done

by an intercomparison of minimum-ionizing particle deposition.

III. DATA COLLECTION, TRIGGERING, PRELIMINARY CUTS

The data for the minimum-bias sample were collected in "minimum-bias runs" with a loose trigger corresponding to an inelastic collision with at least two charged particles in the detector. The high-E_T events were collected with a trigger with 2π coverage in the uranium calorimeter, for laboratory pseudorapidity less than 1. Energy in the NaI was added off line to the energy in the uranium calorimeter. On line, in order to compensate for energy loss in the NaI at the trigger level, the electromagnetic energy seen in the uranium calorimeter modules behind the NaI walls was weighted with an additional factor of 2 in the transverse-energy sums used in the E_T trigger.

For the $\alpha\alpha$ minimum-bias measurements, 83 000 events were collected. For the pp high-E_T samples, 9200 events with $E_T > 28$ GeV in $|y| < 1$ were used. 140 000 events were taken with the AFS field at only 0.1 T (low field) and 80 000 with the standard AFS configuration, a field of 0.5 T (high field.) A comparable sample of events was accumulated with the equipment randomly strobed. These events, used to check for apparent photons in the NaI detector from electronic noise or other sources not associated with events, were an important subtraction for the very-low-transverse-momentum region studied in Ref. 1, but are of only minor importance in the present study, which emphasizes higher transverse momentum and higher-multiplicity events.

IV. ANALYSIS

A. General cuts

A vertex with at least two charged tracks was required in the intersection diamond. The timing of the inner hodoscope and the downstream scintillation counters was required to be consistent with a single interaction. No second event was allowed within ± 200 ns, to reduce effects of pile up in the NaI.

B. Charged-track selection

Charged-track efficiencies were studied, as a function of multiplicity, using the drift-chamber Monte Carlo programs. The efficiencies are shown, for the different data samples, in Fig. 2. The difference in the efficiencies for the different samples reflects the sensitivity of the drift-chamber efficiency to events of different average multiplicity. The charged-track multiplicity for the chamber as a whole was approximately 8 for pp minimum-bias interactions, 11 for $\alpha\alpha$ minimum bias, and 25 for high-E_T events. Studies were done with both loose and strict cuts on recognized tracks and matching between tracks and photons to remove photons associated with tracks. With proper corrections made for differences in cuts, the results were the same, within the quoted systematic errors. The efficiencies shown are for the cuts used in the final analysis. Tracks were required to have at least 30 digitizings in the drift chamber, a χ^2 per degree of freedom of less than 5, pseudorapidity less than 0.8, and center-of-mass azimuthal angle outside of two 23° wedges covering the 16° drift-chamber support gaps in the vertical plane. Electrons were removed from the track sample by a dE/dx cut in the drift chamber for single tracks or by an invariant-mass cut which removed tracks which were members of a pair with mass less than 20 MeV, when assumed to be electrons.

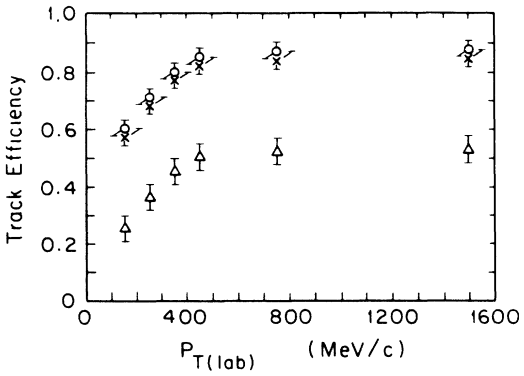

FIG. 2. The track efficiencies after fitting for three different data samples: pp high-field minimum-bias events (crosses), $\alpha\alpha$ minimum-bias events (circles), and pp high-E_T events (triangles).

For the minimum-bias events, as shown in Fig. 3 and discussed more thoroughly in Ref. 1, the charged-particle

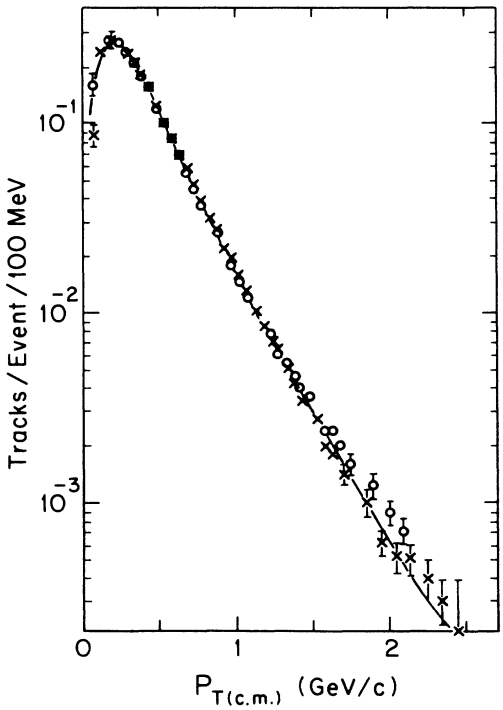

FIG. 3. Observed charged-particle spectra, for minimum-bias events, compared with a parametrization of other measurements (Ref. 12). The ×'s are for the high-field sample; ○'s indicate low field.

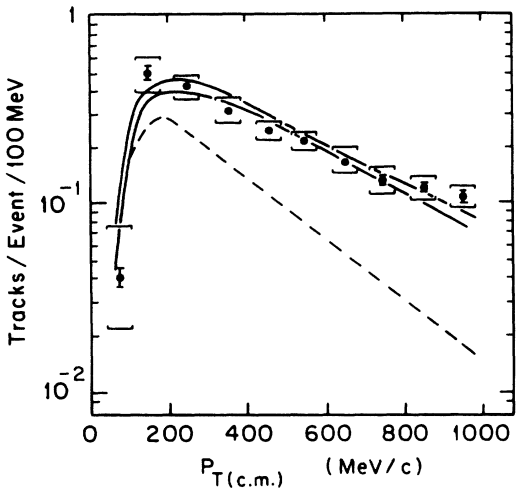

FIG. 4. Observed charged-particle spectra in the high-E_T event sample. The observed spectra are corrected for inefficiencies. Errors shown are statistical. Estimated uncertainities, of approximately 15%, arise from uncertainties in the Monte Carlo modeling of the drift chamber pattern recognition. The dashed line is the minimum-bias parametrization of Ref. 12, as shown in Fig. 3.

spectra and multiplicities are in good agreement with previous measurements.[12] For the high-E_T events, the charged-particle spectra are shown in Fig. 4. The hardening of the high-E_T (>28 GeV), charged-particle spectra compared to the lower-multiplicity event spectra is interpreted as a consequence of the increased importance of hard parton scatters. The band in Fig. 4 shows the range of phenomenological fits used in explaining the charged-particle spectra. The dashed line shows the minimum-bias parametrization from Ref. 12, shown in Fig. 3. The model treats each event as a combination of hard parton scatters and minimum-bias interactions. The shape of the parton scattering is taken from previous jet studies.[13] Energy not used in the parton scattering is partitioned according to minimum-bias measurements at this energy.[12]

C. Photon selection

Raw pulse heights in the NaI crystals were corrected for pedestal shifts and transformed to energy, using individual calibration factors. The raw data were then passed through the standard AFS off-line program chain, including tracking with momentum and vertex determination in the central drift chamber, and shower recognition in the NaI plus uranium calorimeter. For the high-E_T events, only preselected events showing high E_T in the uranium calorimeter ($|y|<1$) were sent on to the NaI reconstruction programs. To see the effect of this high central energy deposition, events with E_T greater than 28 GeV were used, and compared with minimum-bias events.

The NaI pattern-recognition program groups the energy from crystals within a 3×3 crystal matrix into individual showers. Energy and positions are determined through a χ^2 minimization, comparing the observed energy distribution with an average observed lateral shower shape determined using the EGS electromagnetic shower-simulation program[14] on a model of our apparatus. The threshold to trigger a shower definition was 10 MeV. If more than 10 MeV was found adjacent to the 3×3 matrix which defines a shower, overlapping showers were assumed in the χ^2 minimization. Photon candidates were required to be within a fiducial volume of ±53 cm (vertical) by ±34 cm (horizontal) at 113.4 cm from the center of the interaction diamond. Showers which matched a track within an ellipse with axes 8 cm (vertical) by 16 cm (horizontal) were excluded from consideration.[1]

Such close-lying showers were retained as separate showers; their treatment is discussed in detail in Ref. 1. Their inclusion is important mainly at $P_T<100$ MeV. Our present high-multiplicity study is limited to $P_T>100$ MeV/c to minimize systematic effects from showers associated with unrecognized charged particles.

Measurement of the photon spectrum included removal of spurious showers. Our measurements include photons arising from π^0 decay. At these low energies, π^0's have large decay opening angles and yield only one photon in our NaI detector. Spurious photon showers may arise from electronic noise or from unrecognized charged particles. The true observed photons not associated with tracks N_{photon} are given by $N_{\text{photon}}=N_{\text{obs}}-N_{\text{noise}}-N_{\text{unseen tracks}}$, where N_{obs} is the total observed photons not apparently associated with tracks, N_{noise} the apparent photons from electronic noise, and $N_{\text{unseen tracks}}$ the showers associated with charged tracks but with the charged tracks not seen or the photons not properly associated with the charged tracks. The magnitude of the spurious photon showers is shown in Fig. 5 for the final analysis method. Details on the variation of the subtraction of spurious showers for different analysis methods can be found in Refs. 1 and 15. Figure 5 shows that these effects are important below 100 MeV/c and compares the effects for high-E_T and minimum-bias events and for wall 1 and wall 2. The systematic errors here are dominated by knowledge of the charged-track-finding efficiency, and to limit our sensitivity to this source of systematic error we have chosen to report our measurements only above 100 MeV/c.

Subtraction (or exclusion) of false photons from electronic sources was only a small effect for the photons studied in this paper, which have energy in the laboratory system of greater than 100 MeV. Apparent photons from these spurious sources are subtracted using the randomly strobed event sample, as described in Ref. 1. On the other hand, because of the greater number of charged tracks, and because these spurious showers contribute at energies of 50–200 MeV, the proper treatment of these apparent photons was quite important. The background is calculated using the observed response of the NaI detector to charged tracks, together with the drift-chamber tracking inefficiencies calculated from a detector simulation. The charged-track recognition inefficiency, required to give the scale of the subtraction, is input from the drift-chamber Monte Carlo simulation. The procedure was

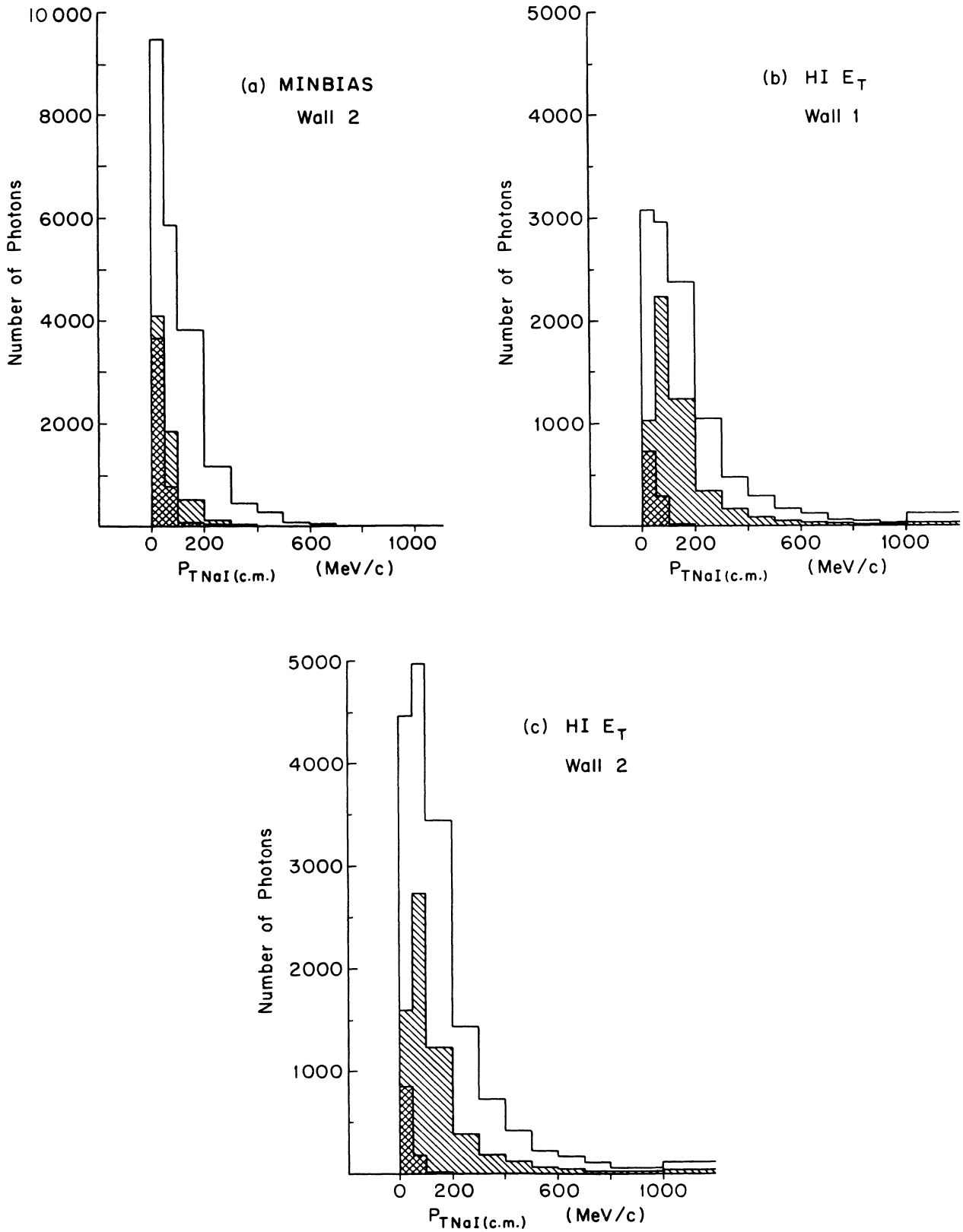

FIG. 5. Observed photon candidates, as a function of P_T. Wall 2 is toward and wall 1 is away from the center-of-mass motion. The cross-hatched region shows the contribution from electronic noise and other sources of signal in randomly strobed events. The shaded area is the contribution from apparent photons arising from showers associated with charged tracks, but for which the tracks were not recognized by the tracking programs. (a) *pp* minimum-bias events, wall 2; (b) *pp* high-E_T events, wall 1; (c) *pp* high-E_T events, wall 2.

followed through with strict matching between tracks and photons and with loose matching. A too strict matching requirement would leave extra photons in the sample, while too loose a requirement would remove more real photons. For each case, appropriate Monte Carlo corrections were made to the final spectrum, using the observed photon and charged-track spectrum. The consistency of the results (to within 15–20%) dominates the systematic limit for our final results.

V. ANALYSIS AND SYSTEMATIC CHECKS

High-multiplicity events provide special challenges for the shower- and track-finding procedures. The charged tracks (charged pions in most cases) are important as a normalization for the photons. Also, at low transverse momenta, showers associated with charged pions can distort the photon spectrum if not properly recognized and removed. The final observed photon spectrum together with the calculated electronic noise and charged-track shower backgrounds are shown in Fig. 5. Figure 5(a) shows the results for wall 2, minimum-bias events; Figs. 5(b) and 5(c) compare the wall 1 and wall 2 high-E_T events.

To test for a change in the photon production relative to the charged tracks, we compare the ratio of the relative photon to charged-particle production between two samples. That is, we first form the ratio (r_{gt}) of photons observed with P_T in a given bin to charged particles observed with P_T in that same bin. Then we plot the ratios of this relative photon to charged-particle production: ($R_{A,B} = r_{gt,\text{sample A}} / r_{gt,\text{sample B}}$).

An indication of the systematic error for the relative γ/charged-track ratio is shown (Fig. 6) by the comparison of the high and low field minimum-bias samples, and the ratio between the two different walls for both the minimum-bias and high-E_T samples. The minimum-bias

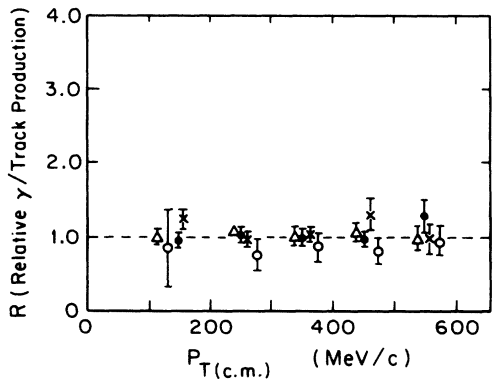

FIG. 6. Relative photon to charged-particle production, compared for different control samples. The ratio between wall 1 and wall 2 is represented for minimum-bias data by dots, for high-field minimum-bias data by crosses and for high E_T by open circles. Triangles show the *pp* minimum-bias high-field-to-low-field comparison. The errors shown include systematic error estimates. Statistical errors dominate only for the high-E_T sample.

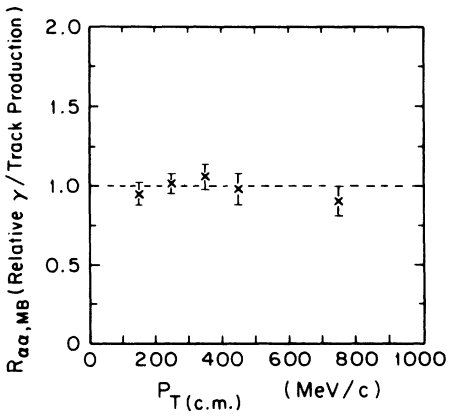

FIG. 7. The ratio $R_{\alpha\alpha,pp\ \text{min bias}}$, a comparison of the photon-to-track ratios.

comparison between low and high field and between wall 1 and wall 2, discussed in more detail in Ref. 15, gives confidence in the method and sets systematic limits on the relative γ/charged-track ratios of approximately 10% at 100 MeV/c, ranging to approximately 20% for $P_T > 500$ MeV/c. The wall 1 and wall 2 comparisons are particularly important in establishing the systematic error limits because of the different average multiplicities in the two walls, due to the center-of-mass Lorentz boost.

VI. $\alpha\alpha$ AND HIGH-E_T COMPARISON TO *pp* MINIMUM-BIAS EVENTS

The final $\alpha\alpha$ and high-E_T comparison results are shown in Figs. 7 and 8. The photon-to-pion ratio for the $\alpha\alpha$ events is seen to be consistent with that in the *pp*

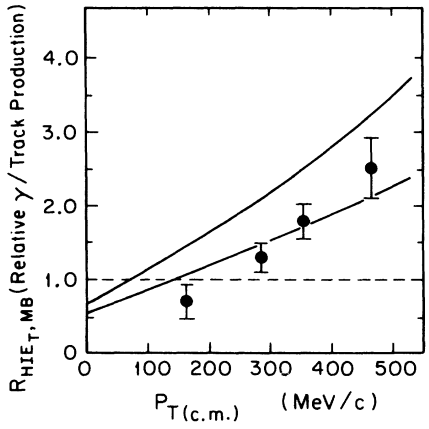

FIG. 8. The ratio of relative gamma to track production for high-E_T to *pp* minimum-bias events. The band shows the expected variation in photon production due to the NaI calorimeter response and the allowed range of parametrizations used to describe the charged-particle spectrum in Fig. 4. The photons are assumed to arise dominantly from π^0's, and the π^0 spectrum is assumed to be the average of the π^+ and π^- spectra. Deviations from the isotopic-spin symmetry assumption give a small effect compared to the other systematic errors.

minimum-bias events, to within the estimated 20% systematic errors, which arise primarily from the charged-track inefficiency corrections.

An enhancement in photon to charged-track production at large P_T is seen (Fig. 8) for high-E_T events, relative to minimum-bias events. The rise is qualitatively understood in terms of the appearance at high P_T of a hard component in the spectrum of pions. Since the photons arise primarily from neutral pion decay, the photons at a given P_T are daughters of π^0's at higher P_T. The photons thus reflect π^0 production at a higher P_T than the P_T of the charged π's with which the photons are compared. The banded curve shows the expected ratio if the π^0 spectrum is assumed to be the same as that of the charged particles shown in Fig. 4. The width of the band arises from the limits in our understanding of the NaI response convoluted with the model limits shown in Fig. 4. The rise is thus consistent with our simple model of the events which overlays a typical "jet" structure arising from a hard scatter with an underlying "minimum bias" event structure. The model fit for π^0's arises entirely from the charged-particle fit shown in Fig. 4, assuming that the π^0 spectrum is the average of the π^+ and π^- spectra. The χ^2 for the γ/π ratio $R_{\mathrm{HI}\,E_T,\mathrm{MB}}$ is 5.9 for 4 degrees of freedom.

Limits on possible direct photon production vary with the form assumed for the direct photon component. Our measurements exclude such a direct component of as much as 19% at the 95% confidence level for a distribution of the form $e^{-P_T/(300\ \mathrm{MeV}/c)}$ and 12% for a distribution $P_T e^{-P_T/(200\ \mathrm{MeV}/c)}$. Figure 9, a plot of the allowed direct photon component at the 95% confidence level, as a function of P_{TAV} in the parametrization $\exp(-P_T/P_{TAV})$, shows that we are insensitive to a direct photon component sharply peaked at low P_T such as that seen in Ref. 2. Although there is some uncertainty in the extrapolation to the photon pole, the appearance of electrons from virtual-photon decay would be expected

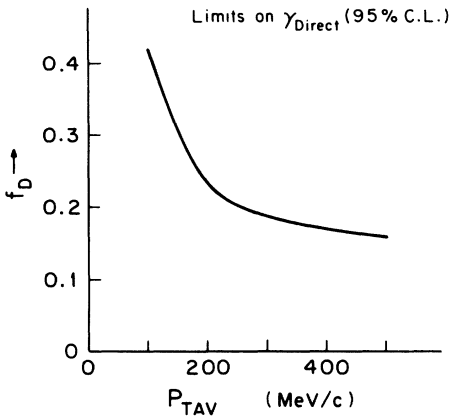

FIG. 9. The allowed percentage direct photon component, compared to all photons expected from decay, defined as a function of P_{TAV}, for the parametrization $\gamma_{\mathrm{direct}} = f_D/P_{TAV} e^{-P_T/P_{TAV}}$.

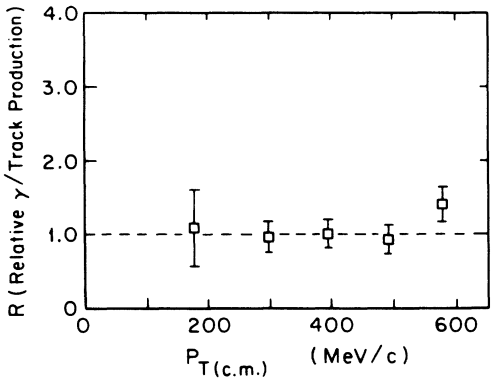

FIG. 10. The ratio $R_{\text{high circularity,low circularity}}$, as described in Fig. 6.

to be suppressed relative to photon production by a factor of approximately α/π, where α is the fine-structure constant.[9] The observed excess of electron pairs[5-7] would then imply, in these models, a real-photon excess of approximately 5% in minimum-bias interactions. If the direct photon component grows quadratically with pion multiplicity, according to the model of Ref. 4, one would then expect a direct photon component of order 10–20% in the high-multiplicity pp events studied here. Thus our limit is just above the overall excess expected from the electron to pion measurements, if the electrons arise from decay of virtual photons.

Another question of interest is whether the relative photon to charged-particle production is different for events with a clear jet structure than in events with a more isotropic E_T, such as might arise from fluctuations in a minimum-bias distribution. To study the photon frequency as a function of the event structure, we used the quantity called circularity, defined as $1-(A-B)/(A+B)$, where A and B are the eigenvalues of the momentum tensor.[16] Small circularity is characteristic of jetlike events, while larger circularities indicate a less collimated structure. The events were divided into high and low circularity. Figure 10 shows the results: these samples are entirely consistent.

Thus, in the P_T range 100–500 MeV/c, no evidence is seen for a direct photon component becoming more important in $\alpha\alpha$ interactions, in high-E_T events, or in more jetlike events. A limit of 19% (95% C.L.) for the appearance of such a directly produced component of the form $e^{-P_T/(300\ \mathrm{MeV}/c)}$ or 12% (95% C.L.) for the form $P_T e^{-P_T/(200\ \mathrm{MeV}/c)}$ in high-multiplicity events is given from our data. These limits are consistent with the hypothesis of a virtual-photon source for low-mass electron pairs.

ACKNOWLEDGMENTS

We would like to thank the Research Councils in our home countries for their support. One of us (J.A.T.) would like to thank M. Jacob and W. H. Lueckenbach for contributions to the analysis and helpful discussions.

[1]T. Åkesson *et al.*, Phys. Rev. D **36**, 2615 (1987).
[2]P. V. Chliapnikov *et al.*, Phys. Lett. **141B**, 276 (1984).
[3]A. T. Goshaw *et al.*, Phys. Rev. Lett. **43**, 1065 (1979).
[4]V. Cerny, P. Lichard, and J. Pisut, Acta Phys. Pol. **B10**, 537 (1979); Phys. Rev. D **24**, 652 (1981); Z. Phys. C **31**, 163 (1986).
[5]T. Åkesson *et al.*, Phys. Lett. **152B**, 411 (1985); Phys. Lett. B **192**, 463 (1987); V. Hedberg, Ph.D. thesis, University of Lund, 1987.
[6]L. Baum *et al.*, Phys. Lett. **60B**, 485 (1976); M. Barone *et al.*, Nucl. Phys. **B132**, 29 (1978); M. Heiden, Ph.D. thesis, Report No. CERN EP 82-05, 1982; M. R. Adams *et al.*, Phys. Rev. D **27**, 1977 (1983).
[7]D. Blockus *et al.*, Nucl. Phys. **B201**, 205 (1982).
[8]J. D. Bjorken and H. Weissberg, Phys. Rev. D **13**, 1405 (1976).
[9]A. Lankford, Ph.D. thesis, Yale University, 1978; N. S. Craigie and D. Schildknecht, Nucl. Phys. **B118**, 311 (1977); N. M. Kroll and W. Wada, Phys. Rev. **98**, 1355 (1955).
[10]H. Gordon *et al.*, Nucl. Instrum. Methods **196**, 303 (1982); O. Botner *et al.*, *ibid.* **196**, 315 (1982); T. Åkesson *et al.*, Phys. Scr. **23**, 649 (1981).
[11]R. Batley *et al.*, Nucl. Instrum. Methods **A242**, 75 (1985).
[12]K. Guettler *et al.*, Nucl. Phys. **B116**, 77 (1976); Phys. Lett. **64B**, 111 (1976); B. Alper *et al.*, Nucl. Phys. **B100**, 237 (1975).
[13]T. Åkesson *et al.*, Z. Phys. C **30**, 27 (1986).
[14]R. L. Ford and W. R. Nelson, Report No. SLAC-210, 1978 (unpublished).
[15]Y. I. Choi, Ph.D. thesis, University of Pittsburgh, 1986.
[16]T. Åkesson *et al.*, Phys. Lett. **128B**, 354 (1983).